ACS APPLIED MATERIALS & INTERFACES

Research Article

www.acsami.org

Size and Surface Functionalization of Iron Oxide Nanoparticles Influence the Composition and Dynamic Nature of Their Protein Corona

Jonathan Ashby,[†] Songqin Pan,[‡] and Wenwan Zhong*[,†]

[†]Department of Chemistry and [‡]Institute for Integrative Genome Biology, University of California, Riverside, California 92521, United States

Supporting Information

ABSTRACT: Nanoparticles (NPs) adsorb proteins when in the biological matrix, and the resulted protein corona could affect NP-cell interactions. The corona has a dynamic nature with the adsorbed proteins constantly exchanging with the free proteins in the matrix at various rates. The rapidly exchanging proteins compose the soft corona, which responds more dynamically to environment changes than the hard corona established by the ones with slow exchange rates. In the present study, the corona formed on the superparamagnetic iron oxide NPs (SPIONs) in human serum was studied by flow field-flow fractionation and ultracentrifugation, which rapidly differentiated the corona proteins based on their exchange rates. By varying the surface hydrophobicity of the SPIONs with a core size around 10 nm, we found out that, the more hydrophobic surface ligand attracted proteins with higher surface hydrophobicity and formed a more dynamic corona with a larger portion of the involved proteins with fast exchange rates. Increasing the core diameter of the SPIONs but keeping the surface ligand the same could also result in a more dynamic corona. A brief investigation of the effect on the cellular uptake of SPIONs using one selected corona protein, transferrin, was conducted. The result showed that, only the stably bound transferrin could significantly enhance cellular uptake, while transferrin bound in a dynamic nature had negligible impact. Our study has led to a better understanding of the relationship between the particle properties and the dynamic nature of the corona, which can help with design of nanomaterials with higher biocompatibility and higher efficacy in biosystems for biomedical applications.

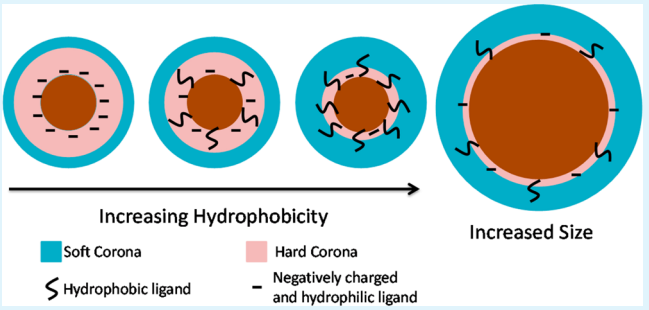

KEYWORDS: *protein corona, protein binding kinetics, surface hydrophobicity, field flow fractionation*

1. INTRODUCTION

Rapidly increasing applications of engineered nanoparticles (NPs) have greatly enhanced the exposure of such materials to all living matters. A better understanding of the behaviors of NPs in biological systems thus becomes imperative for their safe and sustainable implementation.[1,2] It has been established that the protein corona, a layer of proteins adsorbed by the NPs upon their entry into plasma or other protein-containing biological fluids, produces the biological identity of NPs as seen by the cells, affecting the behaviors of NPs in the biological system.[3−7] Not only adsorption of some particular proteins could impact the cellular uptake and biodistribution of NPs;[4,5,7−12] but also the protein corona as a whole could unfavorably block the intended interactions of biofunctionalized NPs with the cell surface receptors.[13,14] Thus, one main focus in corona study has been to determine the corona's composition and find out how the corona composition would be altered by the physicochemical properties of NPs, such as size, shape, and surface chemistry.[3,12,15,16]

With more knowledge about the corona's composition being obtained, the importance of its dynamic nature, the exchange between the bound proteins and free proteins in the environment, has been gradually recognized.[17−22] Those bound with slower exchange kinetics have longer residence time on the NPs, forming the hard corona, and should be more resistant to environmental changes.[23,24] On the other hand, proteins adsorbed to the NPs with faster exchange kinetics establish the less stable, soft corona, and are replaced more quickly by the free proteins in the new environment.[18,23−26] The time- and protein concentration-dependent evolution of the corona was characterized in terms of changes in hydrodynamic size and surface zeta-potential for NPs with various core diameter and surface hydrophobicity.[17,19,27] Changes in corona composition when the NPs moved from plasma to cell cytofluids was also evaluated.[21] Alternatively, the relationship of both the protein binding affinity/kinetics[26,28−30] with particle properties was investigated by using individual

Received: June 20, 2014
Accepted: August 21, 2014
Published: August 21, 2014

protein and NP pairs with techniques like surface plasmon resonance, fluorescence spectroscopy, separation, etc.

However, it remains difficult to obtain a comprehensive image of the dynamic nature of the corona. The biological medium in which the corona is formed could contain over thousands of proteins with large difference in protein concentrations. Protein concentration strongly affects the abundance and exchange rates of the adsorbed proteins in the corona.[23,31] Additionally, the exact contribution of corona protein exchanging kinetics to the biological behaviors of NPs, such as cell uptake and particle distribution, is not clearly known, neither the dependence of the dynamic nature of the corona on the properties of NPs or proteins.

Recently, our group established a method for rapid screening of proteins with distinct exchange kinetics in the corona using ultracentrifugation and flow field-flow fractionation (F4).[32] Centrifugation isolates the entire protein corona for protein identification, with the unbound proteins removed by aliquots of wash solutions. Alternatively, F4 provides a nonequilibrium separation condition[33−35] to cause continuous dissociation of the protein-NP complexes inside the F4 column, and the dissociated proteins are constantly washed away from the complexes by the protein-free mobile phase. Proteins with much slower exchange rates can still be coeluted with the NPs in F4 and identified in the after-column NP collection with significant abundance; while those with much faster exchange kinetics are lost in the column and not detectible in the collection. Thus, by comparing the proteins isolated by centrifugation and F4, we can clearly discern the proteins with very distinct exchange kinetics, and get the snapshots of both the hard and soft corona via only one round of incubation in the complex biological medium.

Herein, with this method to enable simultaneous survey of both the corona composition and its dynamic nature, we studied the protein corona formed on NPs differing in surface coating and particle diameter after incubation with human serum. Changes in the proportion of the hard and soft corona according to the properties of NPs and proteins were investigated to reveal the determinants of corona's dynamic nature. The influence of protein exchanging behavior on cellular uptake was also tested to shed a light on the biological significance of the hard and soft protein coronas.

2. EXPERIMENTAL METHODS

2.1. Reagents. All chemicals used in buffers (sodium phosphate monobasic, sodium phosphate dibasic, FL-70, sodium hydroxide, and ammonium bicarbonate), as well as dithiothreitol, Optima grade water and acetonitrile, were purchased from Fisher Scientific. All proteins used in the study, iodoacetamide and trifluoroacetic acid were purchased from Sigma-Aldrich. Human serum was purchased from Biogenesis (Poole, England). Cell culture media components were purchased from ATCC. Polyacrylic acid and azaleic acid-coated superparamagnetic iron oxide nanoparticles (SPIONS) were prepared in our lab following the protocol developed by the Yin group,[36] and the SPIONs coated with an amphiphilic block copolymer or protein G were purchased from Ocean Nanotech (Springdale, AR).

2.2. Flow Field-Flow Fractionation. For all F4 collections, the conditions were as follows. A F1000 symmetrical F4 instrument (Postnova, Salt Lake City, UT) is coupled to a Shimadzu SP-20A absorbance detector (Columbia, MD). The membrane used was a 10 kDa MWCO regenerated cellulose membrane. The running buffer used in the F4 collections was a 10 mM phosphate buffer (pH 7.5, prepared from monobasic sodium phosphate monohydrate and anhydrous dibasic sodium phosphate solids) with 0.025% FL-70 added. The system was run with channel and cross flows of 0.75 mL/min, with absorbance detection at 280 nm. A graphical description of the F4 operating principles can be found in Supporting Information Figure S1.

2.3. Nanoparticle−Protein Incubation and Isolation. Human serum was first albumin- and IgG-depleted via a depletion kit (Thermo Fisher), and buffer exchanged into 10 mM phosphate with a 7 kDa MWCO Zeba Spin Column (Thermo Fisher). The final concentration was quantified to be 4 mg/mL. Either depleted serum or a 2.5-fold diluted serum (protein concentration was around 6.8 mg/mL) was mixed with an equal volume of the nanoparticle suspension, the particle final concentration being ∼1 μM, and the mixture was incubated for 2 h at 37 °C. For centrifugation-based isolation, samples were diluted to 400 μL in 10 mM phosphate (pH 7.5), and then centrifuged at 16.1 krcf for 0.5 h. After centrifugation, the supernatant was removed. This process was repeated once. For the F4 collections, 4 mL (∼8 min) were collected directly from the detector eluate. Collection windows were determined based on the elution of a nanoparticle control sample. These collections were then concentrated to ∼75 μL using a 4 mL, 10 kDa MWCO Amicon filter (Millipore). Particle-free depleted serum and serum isolations were conducted as a control to identify and eliminate any proteins that naturally precipitated or eluted alongside the SPIONs. All samples were collected in at least triplicate for the purposes of mass spectrometric analysis.

The collected samples underwent standard reduction/alkylation and trypsinization at 37 °C overnight. After digestion, the samples were treated with a 50% acetonitrile solution to denature any adsorbed peptides, and then filtered using a 100 kDa Amicon filter. The peptide-containing filtrate was concentrated to dryness, and reconstituted in 0.1% TFA. These samples then underwent ZipTip desalting and concentration prior to analysis by either 2D MUDPIT LC-nano-MS/MS analysis (Supporting Information Methods) or 1D nano-LC-ESI-MS, using a Waters 2695 separations module interfaced with a Thermo-Finnegan LTQ mass spectrometer. For the depleted serum and serum controls, no proteins were identified with a sufficient confidence score in either the F4 or the centrifugation collections.

2.4. Cellular Uptake of the Nanoparticle−Transferrin Complexes. RAW-Blue mouse macrophage cells were grown in Dulbecco's Modified Eagle Medium supplemented with 10% FBS and 1% penicillin/streptomycin at 95% RH and 3.5% CO_2. Cells were detached from the growth flasks and transferred to 96-well plates at a concentration of 10 000 cells/well. The cells were allowed to grow and adhere for 24 h. The cell culture media was then removed and replaced with a serum-free DMEM. To this, 10 or 25 nm SPIONs with an amphiphilic coating (either neat or incubated with transferrin) were added (giving a final SPION concentration of 150 μg/mL, and a transferrin concentration of 1.875 μM), and the particles incubated for 12h. Cell viability was assayed using the CellTiter 96 Aqueous One Solution cell proliferation assay kit (Promega).

To assess cellular uptake, cells were grown on plate to ∼90% confluence. Afterward, nanoparticle solutions were added similarly to the cell viability test, and allowed to incubate for 2 h. After incubation, the cells were rinsed with serum-free DMEM once. The DMEM was removed, and 100 μL of nitric acid added to each well. The samples were allowed to digest for 18 h. Then, the samples were transferred to 15 mL centrifuge tubes and diluted to 5 mL with 5% nitric acid. After dilution, the iron content in each sample was quantified by inductively coupled plasma-atomic emission spectroscopy (ICP-AES).

3. RESULTS AND DISCUSSION

3.1. Selection of NPs and the Biological Medium. Our study was carried out on superparamagnetic iron oxide NPs (SPIONs), a family of NPs that have showed great potential in biomedical applications.[37,38] Spherical SPIONs with average core diameters between 10 and 25 nm were studied (TEM images shown in Supporting Information Figures S2 and S8). These NPs have comparable dimensions as proteins and are able to escape from opsonization and the reticuloendothelial system.[19] These features allow for longer circulation in the

Table 1. Physical Parameters of the SPIONs Investigated in the Study[a]

NPs	core diameter (nm)	LogP of surface coating	zeta potential (mV)[c]	hydrodynamic diameter (av) (nm)[d]	after DS incubation (nm) (% increase in diameter after incubation)[d]
10-PAA	8.6 ± 2.1	0.67	−45.02 ± 0.74	19	23 (21%)
10-AMP	10 ± 2.5[b]	1.35	−40.43 ± 0.29	15	17 (13%)
10-AZA	12.0 ± 1.4	1.65	−36.13 ± 0.50	14	34 (143%)
10-PrG	10 ± 2.5[b]	N/A	−31.62 ± 0.85	17	25 (47%)
25-AMP	25 ± 2.5[b]	1.35	−40.88 ± 0.21	29	35 (20%)

[a]TEM images of the NPs can be found in Supporting Information Figure S1. [b]Deviations for the core diameters of 10-AMP, 10-PrG, and 25-AMP are maximum tolerances as listed by the supplier. [c]The zeta potentials were from the electrophoretic mobility measured by capillary electrophoresis (Supporting Information). [d]The hydrodynamic diameters of the pristine and serum-incubated SPIONs were calculated from the averaged elution time in F4 (Supporting Information).

body, as well as interactions with biosystems in manners mimicking biomolecules. Thus, understanding the factors that govern corona formation on these SPIONs could help to design more effective biofunctional materials for application in biomedical science.

Three surface ligands were compared: poly(acrylic acid) (PAA), amphiphilic block copolymer (AMP), and azaleic acid (AZA), arranged in order of increasing zeta potential and decreasing hydrophobicity (Table 1). LogP (the logarithm of the partition coefficient between *n*-octanol and water) is an indicator of hydrophobicity, calculated using ALOGPS 2.1 (http://www.vcclab.org).[39,40] The 10 nm SPIONs originally coated with AMP but conjugated to Protein G (PrG) were used to explore bioconjugation's effect on corona formation. To analyze the effect of SPION size on the resulting corona, 25 nm SPIONs coated with AMP were compared to the similarly coated 10 nm SPIONs. In the text below, they were referred as 10-PAA, 10-AZA, 10-AMP, 25-AMP, and 10-PrG, using the core size and the acronym of its surface coating.

In this study, serum depleted of albumin (HSA) and immunoglobulin G (IgG) was used as the biological medium. Depletion of HSA and IgG was to lessen the deviation in dissociation rates caused by their much larger concentrations than other serum proteins; and also to help identify the stronger binders present at lower abundance in serum.[20−22,41,42]

3.2. Corona Formation and Particle Surface Hydrophobicity. Upon incubation with depleted serum, half of the NPs were centrifuged down for coprecipitation of all bound proteins. The other half was injected on the F4 to remove proteins binding with fast exchange kinetics, that is, the soft corona (Figure 1a); leaving only proteins bound with slow exchange kinetics, i.e. the hard corona, to be coisolated with the SPIONs by F4. Proteins collected with the SPIONs were digested and analyzed by 2-dimensional (2D) nano-LC-MS/MS for identification.

The hydrodynamic diameters of the SPIONs before and after serum incubation obtained from the particle retention times in F4 are shown in Table 1. All particle peaks in F4 shifted to later retention times upon serum incubation (Figure 1b for 10-PAA as an example, Supporting Information Figure S3 for other particles), indicating an increase in the overall diameter of the SPIONs. The corresponding size increases ranged from 13% (10-AMP) to 143% (10-AZA).

A selection of proteins coprecipitated with the SPIONs is shown in Table 2. These proteins were normally shared by the coronas formed on several types of the SPIONS studied; and their binding to the SPIONs were particularly discussed in the following text. All identified proteins are listed in Supporting

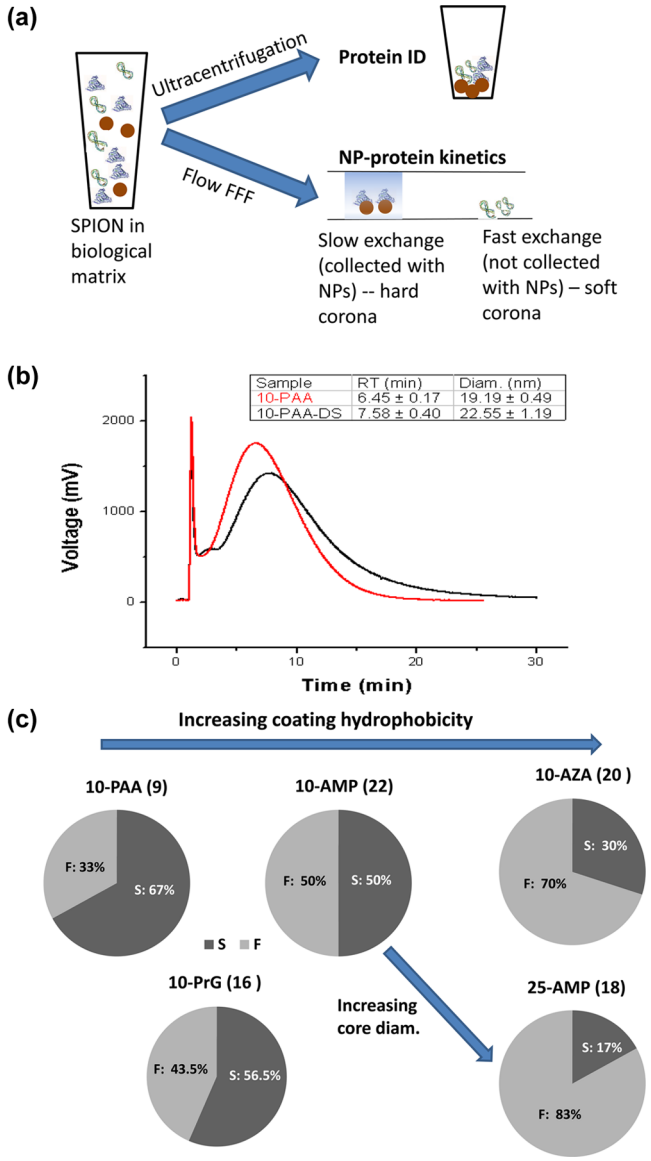

Figure 1. (a) Schematic of the method for determination of the hard and soft protein corona surrounding each particle. (b) F4 fractograms of 10-PAA (red) and 10-PAA incubated with depleted serum (black). The F4 running conditions were stated in Methods. (c) Pie chart indicating the percentage of proteins identified as part of either the hard (dark gray) or soft (light gray) corona surrounding each particle. "S" represents "slow exchange", and "F" is for "fast exchange". The number in the bracket after each NP name was the total number of proteins identified in each particle's corona.

Table 2. Selected Proteins Found in the Coronas of Each Nanoparticle and Indication of Their Relative Exchange Rates[a]

Protein	10-PAA	10-AMP	10-AZA	10-PrG	25-AMP
Alpha-1-antitrypsin	F	S	S	S	-
Alpha-2-macroglobulin	-	S	F	S	S
Haptoglobin	F	S	S	S	S
Transferrin	F	S	F	-	F
Albumin	S	S	F	S	F
Ceruloplasmin	S	S	S	S	F
Complement component 3	S	S	F	S	S
Complement component 4A	-	S	F	-	F
Fetuin A	-	S	-	F	F
Plasminogen	S	F	S	-	F
IgA	-	F	S	S	F
IgG	S	F	-	S	-
IgM	-	F	F	-	F
IgD	-	F	-	-	-
Apolipoprotein AI	-	F	F	F	-
Apolipoprotein B-100	-	F	F	-	-
Apolipoprotein CIII	-	-	F	-	-
Apolipoprotein AIV	-	-	F	-	-
Apolipoprotein D	-	-	F	-	F
Apolipoprotein E	-	-	F	-	-
Alpha-1B-glycoprotein	-	-	-	F	-
Beta-actin	-	-	-	-	F
Gelsolin	-	-	-	F	-
Kinogen-1	-	-	-	F	-
Prealbumin	-	-	-	F	F

[a]F = fast exchange (soft corona; light gray). S = slow exchange (hard corona; dark gray). A full protein list can be found in Supporting Information Table S1.

Information Table S1. While the total number of proteins in the corona on different SPIONs varied, the 10-PAA had the least number of identified proteins. Previous studies on copolymer NPs also observed less protein binding to less hydrophobic particles.[43] Albumin was still present in the corona of all particles, although the majority of it should have been removed before incubation with the SPIONs. Several apolipoproteins, previously reported to bind to NPs of different materials and sizes,[3,43] also bound to our SPIONs with the exception of 10-PAA. In particular, the 10-AZA, the SPION with the most hydrophobic surface ligand, adsorbed the highest number of apolipoproteins compared to other SPIONs.[21,23,43]

We grouped the bound proteins into either slow (S, dark gray blocks in Table 2; collected by both centrifugation- and F4-based isolation) or fast (F, light gray blocks in Table 2; only found by centrifugation-based isolation) exchange kinetics via comparison of proteins collected by centrifugation and F4. Reliability of the bulk media kinetics assignment was confirmed by analyzing the binding behaviors of selected protein−particle pairs with the standard methods: SDS-PAGE and capillary electrophoresis (Supporting Information Figures S4 and S5). Distribution of the dark and light gray colors in Table 2 hints that the more hydrophobic surface ligand probably recruited more rapidly exchanging proteins to the corona. To confirm this, the percentages of the slow or fast exchanging proteins in the corona were compared across all particles. The results were plotted in the form of pie charts in Figure 1c. It is clearly seen that, as surface ligand hydrophobicity increased a more dynamic corona would be formed, recruiting a larger portion of the rapidly exchanging proteins. The pie charts also showed similar proportions of the proteins with fast and slow exchange rates on the 10-PrG compared to that on the 10-AMP, meaning that both particles had coronas with comparable dynamic nature.

3.3. Dynamic Nature of Corona and Protein Hydrophobicity. Grand average of hydropathy (GRAVY) scores of the proteins were calculated using ProtParam, a tool available in the SIB ExPASy Bioinformatics Resources Portal.[44] A less negative GRAVY score represents a more hydrophobic nature of the protein. The GRAVY score obtained from the full sequences of the corona did not show any trend among different types of the SPIONs, nor did other comparisons such as pI (Supporting Information Figure S6). Alternatively, we compared the averaged surface GRAVY scores of the corona proteins on each type of the SPIONs. GETAREA, a software algorithm for calculation of solvent accessible surface areas, was used to identify the amino acid residues of each protein that had greater than 50% surface accessibility; and these residues were then used to calculate the surface GRAVY score.[45]

Among the 10 nm SPIONs, the corona's surface GRAVY score became less negative as the hydrophobicity of the surface ligand increased (Figure 2a). This means that the hydrophobic

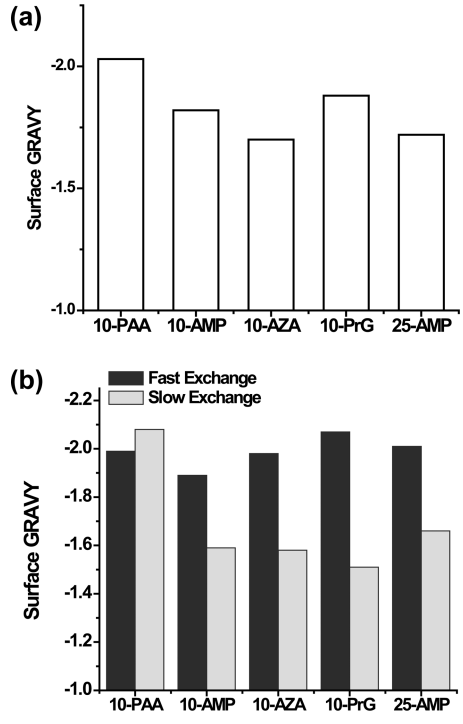

Figure 2. (a) Comparison of average surface GRAVY scores comprising each SPION-protein corona. Surface GRAVY scores were obtained by manually averaging the GRAVY scores of surface-accessible residues for each protein. A more positive GRAVY score indicates a more hydrophobic average protein surface. (b) Comparison of the average surface GRAVY for the proteins with slow exchange rates (hard corona, dark gray) and fast exchange rates (soft corona, light gray).

particle surface attracts not only the lipophilic apolipoproteins but also favors proteins with high surface hydrophobicity. Similar to Figure 1c, the surface GRAVY score of the 10-PrG corona again is comparable to that of the 10-AMP. PrG is quite hydrophilic with a GRAVY score of −0.514, and carries negative charge under physiological pH with a pI of 4.6. However, its corona contains proteins specific to PrG and the corona property cannot be simply judged by surface hydro-

phobicity and charge. The specific recruitment of proteins with higher surface hydrophobicity to the hydrophobic particle surface tells us that, the main driving force for protein adsorption on the SPIONs is hydrophobic interaction. The hydrophobic portion of the particle surface ligand clustered with the hydrophobic patches on the protein surface to reduce interaction with water molecules. Such clustering assembled the protein−NP complex and the assembly could be stabilized by increase in entropy.[46] Indeed, disruption in protein conformation was observed in those bound to the SPIONs with slow exchange kinetics, that is, high stability, but not in those with fast exchange kinetics, as seen in circular dichroism (CD) experiments.[32,47,48]

Moreover, in the corona of all SPIONs studied, the surface GRAVY scores of proteins belonging to the slow exchange kinetics category were more negative than those with fast exchange kinetics, with the 10-PAA as the only exception (Figure 2b). The higher adsorption stability of the more hydrophilic proteins on particle surface could be because they established stronger H-bonding and dipole−dipole interactions with the surface than the more hydrophobic proteins, which limited the fluctuation of the protein−NP assembly.[49] The proteins with fast and slow exchange kinetics in the corona of the 10-PAA had similar surface GRAVY scores. The interaction with the 10-PAA was believed to be stabilized by the size of proteins, achieving stronger dispersion force: the average Mw of the slow exchanging proteins on the 10-PAA was significantly (two-sample t test at the 0.05 level) higher than that of the fast exchanging proteins (Supporting Information Figure S7).

3.4. Impacts from Particle Diameter on Corona Formation. The types of proteins and their binding kinetics on the 10-AMP were significantly different than that on the 25-AMP. For instance, apolipoprotein AI (Apo A-I), the major component of the high density lipoprotein (HDL) particle, was bound to 10-AMP but not to the 25-AMP. In fact, Apo A-I bound to all 10 nm SPIONs except for 10-PAA. ApoA-I is the major component in the spherical HDL species with diameters ranging from 7 to 12 nm and could form ring-shaped dimers to wrap around the lipid bilayer core.[50,51] Hence, it is feasible for this protein to selectively bind to a nanomaterial of similar dimensions to HDL.

In the corona of the 25-AMP, 81% of the total proteins had fast exchange kinetics, which is much higher than the 50% seen in 10-AMP (Figure 1c). The more dynamic corona on the larger SPIONs was also confirmed using a 15 nm SPION coated with the same amphiphilic polymer as the 10- and 25-AMP (15-AMP), carried a similar zeta-potential of -41.15 ± 0.21 mV to those two, and had the intermediate core (15 nm, Supporting Information Figure S8 for TEM image) and hydrodynamic (19 nm) sizes. The F4 fractograms of 15-AMP and 15-AMP incubated with depleted serum can be found in Supporting Information Figure S8b. Its intermediate size then led to an intermediate percentage (72%) of the proteins with fast exchange kinetics in their corona (Supporting Information Figure S8 and Table S1 for the identified proteins). Such an impact on the dynamic nature of the protein corona from particle size could arise from the flatter surface curvature of the larger particles that makes it harder for proteins to adapt. Lower disturbance to the protein structure was induced. As a result, the proteins would dissociate more quickly from a flatter surface, compared to from a surface with sharper curvature as on the smaller particles.[52,53]

The larger 25-AMP also bound to proteins with a less negative average surface GRAVY score, that is, proteins with higher hydrophobicity, compared to the 10-AMP (Figure 2a). Similar to the smaller SPIONs, proteins with slow exchange kinetics in the corona of the 25-AMP were more hydrophilic than those with fast exchange kinetics (Figure 2b). This could be attributed to the more difficult adaptation to the NP surface which then required the proteins to have higher surface hydrophobicity in order to be adsorbed. Our study used NPs at the same particle molar concentration at the incubation. The 25-AMP had a larger total surface area than the smaller 10-AMP to provide larger interface for dewetting of the hydrophobic protein surface, facilitating the binding of the more hydrophobic proteins.[46] Still, larger protein Mw could further stabilize the interaction, as in the case of the 10-PAA: proteins with slow exchange kinetics when binding to the 25-AMP had a relatively larger average Mw than those with fast exchange kinetics (Supporting Information Figure S7).

In addition to incubation with the depleted serum, the 25-AMP was also incubated with 5-fold diluted whole serum to see how protein complexity and concentration would affect the dynamic feature of the corona. The protein content in this 5-fold dilution was around 3.4 mg/mL, higher than the 2 mg/mL of the depleted serum in the incubation (Supporting Information Figure S9a). Supporting Information Figure S9b displayed the fractograms collected after serum incubation. The calculated diameter for the 25-AMP in the serum with higher protein contents increased to 50 nm (79% size increase), significantly larger than the size increase in the depleted serum. In addition, there were some new fast exchange-interacting proteins (Supporting Information Table S1). A handful of proteins (albumin, A1AT, and IgA/G/M) were also found to shift from fast exchange to slow exchange because of the large increase in these proteins' concentrations. Still, the percentage of fast exchange interactions remained high (64%), indicating that, even in serum, there is still a correlation found between the SPIONs size and the dynamics of the SPION-protein corona.

Overall, our results support the hypothesis that the composition and dynamic nature of the SPION-protein corona has a large dependence not only on the surface coating of the nanoparticle, but its size as well.

3.5. Change of the Dynamic Nature of Corona with Bioconjugation. The 10-PrG was produced by linking protein G to the AMP coating on the 10-AMP. By attributing the proteins with slow exchange kinetics to the hard corona, and those with fast exchange kinetics to the soft corona, we compared the percentages of proteins remained in the hard or soft corona upon conjugation of protein G (Figure 3). More than 65% of the proteins in the hard corona of the 10-PrG were the same ones found in the hard corona of the 10-AMP. But more than 70% of the proteins in the soft corona of the 10-PrG were new proteins not found in either the hard or soft corona of the 10-AMP. IgA and IgG were counted as the new proteins added to the hard corona because of specific interaction with PrG. Fetuin A, another major carrier protein in serum, changed from a stably bound protein on the 10-AMP to a rapidly exchanging protein on the 10-PrG.

Our results illustrated an interesting phenomenon: rather than the composition of the hard corona be dependent solely on the biomolecule conjugated to the nanoparticle, the hard corona is instead a mixture of proteins specific to both the bioconjugate and the surface coating. This has implications for

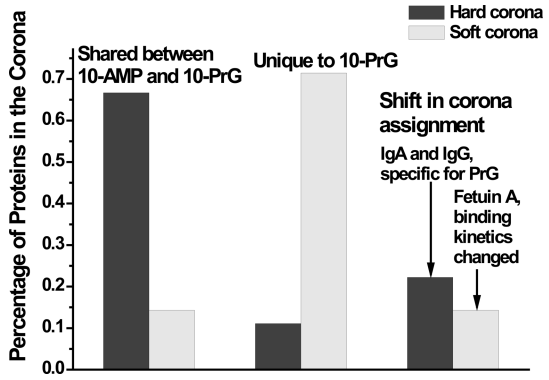

Figure 3. Comparison of similar and unique proteins in the protein coronas for 10-AMP and 10-PrG. L−R: Proteins in each corona shared between the two particles, proteins in each corona unique to 10-PrG, and proteins in each corona that were previously known to bind to protein G.

affinity purification-mass spectrometry; the initial surface coating should be carefully considered to understand and control the degree of nonspecific interactions seen.

3.6. Effects of the Protein Binding Nature on Cellular Uptake. It is believed that proteins in the hard corona would mediate cell−particle interaction but no direct evidence has been provided in previous corona studies. Hence, we tested the uptake of the 10- and 25-AMP carrying transferrin by the RAW-Blue mouse macrophages. As reported in Table 2, the 10-AMP binds to transferrin stably, while transferrin bound to the 25-AMP with fast exchange rates. The macrophages were incubated with 10- and 25-AMP, with or without preincubation with transferrin for overnight in serum-free media. A cell viability test proved that the concentration of NPs used imposed very low toxicity to the cells (Figure 4a). Inductively coupled plasma-atomic emission spectroscopy (ICP-AES) was employed to test the iron content in the cells after incubation with the AMP-coated particles and the transferrin-bound ones (Figure 4b). Both 10-AMP and 25-AMP had similar cellular uptake in the absence of transferrin. The presence of transferrin, however, almost doubled the uptake of 10-AMP into the cells (29−43%), but not affecting the uptake of 25-AMP (33−29%). As anticipated, proteins with fast exchange rates had less influence on the interaction of NPs with cells than the stably bound proteins. Although this is a preliminary study comprising a single protein, our result points out the necessity of forming a stable conjugate with proteins, if the cell receptor-protein interaction is required for carrying out the biological functions of the NPs.

4. CONCLUSIONS

In our study, various carrier proteins like albumin, components of the complement system, and apolipoproteins were found to bind to the negatively charged SPIONs. A corona containing such proteins on the SPIONs may increase their circulation time, make them potential activators to the complement pathways, or enable mimicking of the behaviors of the high- or low-density lipoprotein particles. However, these proteins interacted with the SPIONs at different association/dissociation rates, which may impact their contribution to the biological behaviors of the SPIONs.

Our brief cell uptake experiment hints that, the proteins stably adsorbed would affect cellular uptake more significantly than those bound more dynamically. This may be the reason

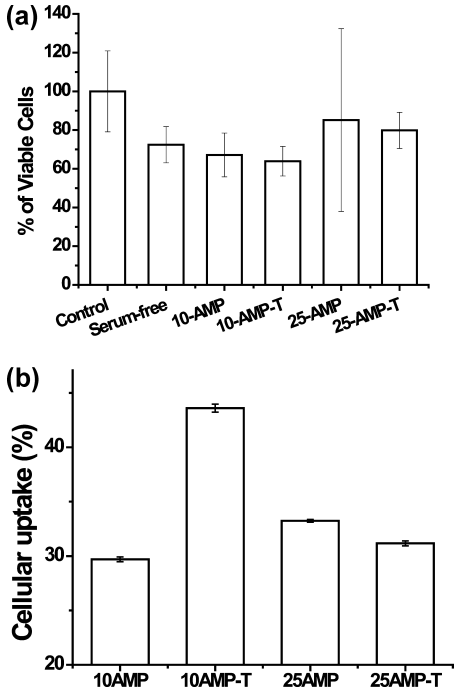

Figure 4. (a) Cell viability of RAW-Blue mouse macrophage cells when incubated with SPION for 16 h. (b) Cellular uptake of SPIONS after 4 h incubation. Iron content was determined by ICP-AES. Control: DMEM with 10% FBS. Serum-free: DMEM only, no FBS. 10,25-AMP: SPION incubated in serum-free DMEM. 10,25-AMP-T: SPION preincubated with transferrin prior to incubation with cells in serum-free DMEM. 10-AMP-T is a slow-dissociation complex, while 25-AMP-T is a fast-dissociation complex.

why some protein corona could diminish the targeting capability of the biofunctionalized NPs, as reported by Salvati et al.[14] On the contrary, the quickly exchanging proteins could reach binding equilibrium more rapidly than the ones with slow exchange kinetics, and rapidly mask the surface of the nanomaterials upon entry to the biological medium. They may contribute more to elongating the circulation time of NPs, reducing the toxicity originated from particle dissolution and high surface activity, and bypassing transportation barriers. Our analysis of the corona on the 10-PrG revealed that, the majority of the hard corona formed on the base NPs remained in the corona of the bioconjugated particles. Thus, careful consideration of the corona property of the base particle is necessary in preparation of the functional NPs.

For the carboxylated SPIONs used in our study, a ligand having higher hydrophobicity or a larger particle diameter would be referred, because both would lead to a more dynamic corona.

On the other hand, to stabilize the hydrophobic interaction between our SPIONs and the serum proteins, strong H-bonding and dipole−dipole interaction at the interface should be established, which would rely on the amino acid side chains and surface ligand structure at the interface.[54,55] In addition, feasible adaptation of the protein onto the NP surface is important, like in the case of Apo A-I preferentially binding to the 10 nm SPIONs but not the 25 nm particles. Better fitting to the surface curvature could increase the area of binding interface, causing the release of more water molecules and the deformation of protein structure. Both effects could enhance

the system entropy to gain more reduction in the system free energy upon binding.

■ ASSOCIATED CONTENT

Supporting Information

Methods used for protein identification, F4 fractograms, a table of corona proteins for each particle, confirmation of SPION-protein kinetics, analysis of physical parameters for each protein corona, serum incubations of nanomaterials. This material is available free of charge via the Internet at http://pubs.acs.org.

■ AUTHOR INFORMATION

Corresponding Author

*E-mail: wenwan.zhong@ucr.edu.

Notes

The authors declare no competing financial interest.

■ ACKNOWLEDGMENTS

This work was supported by National Institute of Environmental Health Sciences Grant No. 1R21ES017870-01A1 and by National Science Foundation CAREER Grant No. 1057113. Jonathan Ashby was supported by the National Science Foundation Graduate Research Fellowship under Grant Number DGE-0813967. The authors are also very grateful for the support of Dr. Yadong Yin on SPION synthesis, as well as UCR's Institute for Integrative Genome Biology for the usage of the Typhoon imager and MUDPIT analysis.

■ REFERENCES

(1) Sadik, O. A.; Zhou, A. L.; Kikandi, S.; Du, N.; Wang, Q.; Varner, K. Sensors as Tools for Quantitation, Nanotoxicity and Nano-monitoring Assessment of Engineered Nanomaterials. *J. Environ. Monit.* **2009**, *11*, 1782−1800.

(2) Schulze, C.; Kroll, A.; Lehr, C. M.; Schafer, U. F.; Becker, K.; Schnekenburger, J.; Isfort, C. S.; Landsiedel, R.; Wohlleben, W. Not Ready to Use—Overcoming Pitfalls When Dispersing Nanoparticles in Physiological Media. *Nanotoxicology* **2008**, *2*, 51−U17.

(3) Lundqvist, M.; Stigler, J.; Elia, G.; Lynch, I.; Cedervall, T.; Dawson, K. A. Nanoparticle Size and Surface Properties Determine the Protein Corona with Possible Implications for Biological Impacts. *Proc. Natl. Acad. Sci. U. S. A.* **2008**, *105*, 14265−14270.

(4) Lynch, I.; Dawson, K. A. Protein−Nanoparticle Interactions. *Nano Today* **2008**, *3*, 40−47.

(5) Monopoli, M. P.; Aberg, C.; Salvati, A.; Dawson, K. A. Biomolecular Coronas Provide the Biological Identity of Nanosized Materials. *Nat. Nanotechnol.* **2012**, *7*, 779−786.

(6) Zeineldin, R.; Al-Haik, M.; Hudson, L. G. Role of Polyethylene Glycol Integrity in Specific Receptor Targeting of Carbon Nanotubes to Cancer Cells. *Nano Lett.* **2009**, *9*, 751−757.

(7) Nel, A. E.; Madler, L.; Velegol, D.; Xia, T.; Hoek, E. M. V.; Somasundaran, P.; Klaessig, F.; Castranova, V.; Thompson, M. Understanding Biophysicochemical Interactions at the Nano-Bio Interface. *Nat. Mater.* **2009**, *8*, 543−557.

(8) Keck, C. M.; Jansch, M.; Mueller, R. H. Protein Adsorption Patterns and Analysis on IV Nanoemulsions—The Key Factor Determining the Organ Distribution. *Pharmaceutics* **2013**, *5*, 36−68.

(9) Kreuter, J.; Alyautdin, R. N.; Kharkevich, D. A.; Ivanov, A. A. Passage of Peptides Through the Blood−Brain Barrier with Colloidal Polymer Particles (Nanoparticles). *Brain Res.* **1995**, *674*, 171−174.

(10) Moghimi, S. M.; Muir, I. S.; Illum, L.; Davis, S. S.; Kolbbachofen, V. Coating Particles with a Block-Copolymer (Polyoxamine-908) Suppresses Opsonization but Permits the Activity of Dysopsonins in the Serum. *Biochim. Biophys. Acta* **1993**, *1179*, 157−165.

(11) Ogawara, K.; Furumoto, K.; Nagayama, S.; Minato, K.; Higaki, K.; Kai, T.; Kimura, T. Pre-coating with Serum Albumin Reduces Receptor-Mediated Hepatic Disposition of Polystyrene Nanosphere: Implications for Rational Design of Nanoparticles. *J. Controlled Release* **2004**, *100*, 451−455.

(12) Walkey, C. D.; Olsen, J. B.; Guo, H. B.; Emili, A.; Chan, W. C. W. Nanoparticle Size and Surface Chemistry Determine Serum Protein Adsorption and Macrophage Uptake. *J. Am. Chem. Soc.* **2012**, *134*, 2139−2147.

(13) Patel, P. C.; Giljohann, D. A.; Daniel, W. L.; Zheng, D.; Prigodich, A. E.; Mirkin, C. A. Scavenger Receptors Mediate Cellular Uptake of Polyvalent Oligonucleotide-Functionalized Gold Nanoparticles. *Bioconj.Chem.* **2010**, *21*, 2250−2256.

(14) Salvati, A.; Pitek, A. S.; Monopoli, M. P.; Prapainop, K.; Bombelli, F. B.; Hristov, D. R.; Kelly, P. M.; Aberg, C.; Mahon, E.; Dawson, K. A. Transferrin-Functionalized Nanoparticles Lose Their Targeting Capabilities When a Biomolecule Corona Adsorbs on the Surface. *Nat. Nanotechnol.* **2013**, *8*, 137−143.

(15) Gref, R.; Luck, M.; Quellec, P.; Marchand, M.; Dellacherie, E.; Harnisch, S.; Blunk, T.; Muller, R. H. "Stealth" Corona-Core Nanoparticles Surface Modified by Polyethylene Glycol (PEG): Influences of the Corona (PEG Chain Length and Surface Density) and of the Core Composition on Phagocytic Uptake and Plasma Protein Adsorption. *Colloid Surf., B* **2000**, *18*, 301−313.

(16) Tenzer, S.; Docter, D.; Rosfa, S.; Wlodarski, A.; Kuharev, J.; Rekik, A.; Knauer, S. K.; Bantz, C.; Nawroth, T.; Bier, C.; Sirirattanapan, J.; Mann, W.; Treuel, L.; Zellner, R.; Maskos, M.; Schild, H.; Stauber, R. H. Nanoparticle Size Is a Critical Physicochemical Determinant of the Human Blood Plasma Corona: A Comprehensive Quantitative Proteomic Analysis. *ACS Nano* **2011**, *5*, 7155−7167.

(17) Caracciolo, G.; Pozzi, D.; Capriotti, A. L.; Cavaliere, C.; Foglia, P.; Amenitsch, H.; Lagana, A. Evolution of the Protein Corona of Lipid Gene Vectors as a Function of Plasma Concentration. *Langmuir* **2011**, *27*, 15048−15053.

(18) Casals, E.; Pfaller, T.; Duschl, A.; Oostingh, G. J.; Puntes, V. Time Evolution of the Nanoparticle Protein Corona. *ACS Nano* **2010**, *4*, 3623−3632.

(19) Casals, E.; Pfaller, T.; Duschl, A.; Oostingh, G. J.; Puntes, V. F. Hardening of the Nanoparticle-Protein Corona in Metal (Au, Ag) and Oxide (Fe_3O_4, CoO, and CeO_2) Nanoparticles. *Small* **2011**, *7*, 3479−3486.

(20) Dell'Orco, D.; Lundqvist, M.; Oslakovic, C.; Cedervall, T.; Linse, S. Modeling the Time Evolution of the Nanoparticle−Protein Corona in a Body Fluid. *PLoS One* **2010**, *5*, 8.

(21) Lundqvist, M.; Stigler, J.; Cedervall, T.; Berggard, T.; Flanagan, M. B.; Lynch, I.; Elia, G.; Dawson, K. The Evolution of the Protein Corona around Nanoparticles: A Test Study. *ACS Nano* **2011**, *5*, 7503−7509.

(22) Sahneh, F. D.; Scoglio, C.; Riviere, J. Dynamics of Nanoparticle−Protein Corona Complex Formation: Analytical Results from Population Balance Equations. *PLoS One* **2013**, *8*, 10.

(23) Monopoli, M. P.; Walczyk, D.; Campbell, A.; Elia, G.; Lynch, I.; Bombelli, F. B.; Dawson, K. A. Physical-Chemical Aspects of Protein Corona: Relevance to in Vitro and in Vivo Biological Impacts of Nanoparticles. *J. Am. Chem. Soc.* **2011**, *133*, 2525−2534.

(24) Walczyk, D.; Bombelli, F. B.; Monopoli, M. P.; Lynch, I.; Dawson, K. A. What the Cell "Sees" in Bionanoscience. *J. Am. Chem. Soc.* **2010**, *132*, 5761−5768.

(25) Casals, E.; Puntes, V. F. Inorganic Nanoparticle Biomolecular Corona: Formation, Evolution and Biological Impact. *Nanomedicine* **2012**, *7*, 1917−1930.

(26) Cedervall, T.; Lynch, I.; Lindman, S.; Berggard, T.; Thulin, E.; Nilsson, H.; Dawson, K. A.; Linse, S. Understanding the Nanoparticle−Protein Corona Using Methods to Quantify Exchange Rates and Affinities of Proteins for Nanoparticles. *Proc. Natl. Acad. Sci. U. S. A.* **2007**, *104*, 2050−2055.

(27) Chen, R.; Choudhary, P.; Schurr, R. N.; Bhattacharya, P.; Brown, J. M.; Ke, P. C. Interaction of Lipid Vesicle with Silver Nanoparticle−Serum Albumin Protein Corona. *Appl. Phys. Lett.* **2012**, *100*, 4.

(28) Li, L. W.; Mu, Q. X.; Zhang, B.; Yan, B. Analytical Strategies for Detecting Nanoparticle−Protein Interactions. *Analyst* **2010**, *135*, 1519−1530.
(29) Canovi, M.; Lucchetti, J.; Stravalaci, M.; Re, F.; Moscatelli, D.; Bigini, P.; Salmona, M.; Gobbi, M. Applications of Surface Plasmon Resonance (SPR) for the Characterization of Nanoparticles Developed for Biomedical Purposes. *Sensors* **2012**, *12*, 16420−16432.
(30) Li, N.; Zeng, S.; He, L.; Zhong, W. Probing Nanoparticle−Protein Interaction by Capillary Electrophoresis. *Anal. Chem.* **2010**, *82*, 7460−7466.
(31) Ghavami, M.; Saffar, S.; Abd Emamy, B.; Peirovi, A.; Shokrgozar, M. A.; Serpooshan, V.; Mahmoudi, M. Plasma Concentration Gradient Influences the Protein Corona Decoration on Nanoparticles. *RSC Adv.* **2013**, *3*, 1119−1126.
(32) Ashby, J.; Schachermeyer, S.; Pan, S. Q.; Zhong, W. W. Dissociation-Based Screening of Nanoparticle−Protein Interaction via Flow Field-Flow Fractionation. *Anal. Chem.* **2013**, *85*, 7494−7501.
(33) Berezovski, M.; Krylov, S. N. Nonequilibrium Capillary Electrophoresis of Equilibrium Mixtures—A Single Experiment Reveals Equilibrium and Kinetic Parameters of Protein−DNA Interactions. *J. Am. Chem. Soc.* **2002**, *124*, 13674−13675.
(34) Krylov, S. N. Nonequilibrium Capillary Electrophoresis of Equilibrium Mixtures (NECEEM): A Novel Method for Biomolecular Screening. *J. Biomol. Screening* **2006**, *11*, 115−122.
(35) Krylova, S. M.; Dove, P. M.; Kanoatov, M.; Krylov, S. N. Slow-Dissociation and Slow-Recombination Assumptions in Nonequilibrium Capillary Electrophoresis of Equilibrium Mixtures. *Anal. Chem.* **2011**, *83*, 7582−7585.
(36) Ge, J. P.; Hu, Y. X.; Biasini, M.; Dong, C. L.; Guo, J. H.; Beyermann, W. P.; Yin, Y. D. One-Step Synthesis of Highly Water-Soluble Magnetite Colloidal Nanocrystals. *Chem.—Eur. J.* **2007**, *13*, 7153−7161.
(37) Kouassi, G. K. Magnetic and Gold-Coated Magnetic Iron Oxide Nanoparticles as Detection Tools: Preparation, Characterization, and Biosensing Applications. *Curr. Nanosci.* **2011**, *7*, 510−523.
(38) Liu, F. J.; Laurent, S.; Fattahi, H.; Elst, L. V.; Muller, R. N. Superparamagnetic Nanosystems Based on Iron Oxide Nanoparticles for Biomedical Imaging. *Nanomedicine* **2011**, *6*, 519−528.
(39) Tetko, I. V.; Tanchuk, V. Y. Application of Associative Neural Networks for Prediction of Lipophilicity in ALOGPS 2.1 Program. *J. Chem. Inf. Model.* **2002**, *42*, 1136−1145.
(40) Tetko, I. V.; Gasteiger, J.; Todeschini, R.; Mauri, A.; Livingstone, D.; Ertl, P.; Palyulin, V.; Radchenko, E.; Zefirov, N. S.; Makarenko, A. S.; Tanchuk, V. Y.; Prokopenko, V. V. Virtual Computational Chemistry Laboratory—Design and Description. *J. Comput.-Aided Mol. Des.* **2005**, *19*, 453−463.
(41) Vroman, L.; Adams, A. L. Adsorption of Proteins out of Plasma and Solutions in Narrow Spaces. *J. Colloid Interface Sci.* **1986**, *111*, 391−402.
(42) Vroman, L.; Adams, A. L.; Fischer, G. C.; Munoz, P. C. Interaction of High Molecular-Weight Kininogen, Factor-XII, and Fibrinogen in Plasma at Interfaces. *Blood* **1980**, *55*, 156−159.
(43) Cedervall, T.; Lynch, I.; Foy, M.; Berggard, T.; Donnelly, S. C.; Cagney, G.; Linse, S.; Dawson, K. A. Detailed Identification of Plasma Proteins Adsorbed on Copolyer Nanoparticles. *Angew. Chem. Int. Ed.* **2007**, *46*, 5754−5756.
(44) Gasteiger, E.; Gattiker, A.; Hoogland, C.; Ivanyi, I.; Appel, R. D.; Bairoch, A. ExPASy: The Proteomics Server for In-Depth Protein Knowledge and Analysis. *Nucleic Acids Res.* **2003**, *31*, 3784−3788.
(45) Fraczkiewicz, R.; Braun, W. Exact and Efficient Analytical Calculation of the Accessible Surface Areas and Their Gradients for Macromolecules. *J. Comput. Chem.* **1998**, *19*, 319−333.
(46) Chandler, D. Interfaces and the Driving Force of Hydrophobic Assembly. *Nature* **2005**, *437*, 640−647.
(47) Billsten, P.; Wahlgren, M.; Arnebrant, T.; McGuire, J.; Elwing, H. Structural-Changes of T4 Lysozyme Upon Adsorption to Silica Nanoparticles Measured by Circular-Dichroism. *J. Colloid Interface Sci.* **1995**, *175*, 77−82.
(48) Laera, S.; Ceccone, G.; Rossi, F.; Gilliland, D.; Hussain, R.; Siligardi, G.; Calzolai, L. Measuring Protein Structure and Stability of Protein−Nanoparticle Systems with Synchrotron Radiation Circular Dichroism. *Nano Lett.* **2011**, *11*, 4480−4484.
(49) ten Wolde, P. R.; Chandler, D. Drying-Induced Hydrophobic Polymer Collapse. *Proc. Natl. Acad. Sci. U.S.A.* **2002**, *99*, 6539−6543.
(50) Vedhachalam, C.; Sevugan Chetty, P.; Nickel, M.; Dhanasekaran, P.; Lund-Katz, S.; Rothblat, G. H.; Phillips, M. C. Influence of Apolipoprotein (Apo) A−I Structure on Nascent High Density Lipoprotein (HDL) Particle Size Distribution. *J. Biol. Chem.* **2010**, *285*, 31965−31973.
(51) Silva, R. A. G. D.; Huang, R.; Morris, J.; Fang, J.; Gracheva, E. O.; Ren, G.; Kontush, A.; Jerome, W. G.; Rye, K.-A.; Davidson, W. S. Structure of Apolipoprotein A−I in Spherical High Density Lipoproteins of Different Sizes. *Proc. Natl. Acad. Sci. U. S. A.* **2008**, *105*, 12176−12181.
(52) Tsai, D. H.; DelRio, F. W.; Keene, A. M.; Tyner, K. M.; MacCuspie, R. I.; Cho, T. J.; Zachariah, M. R.; Hackley, V. A. Adsorption and Conformation of Serum Albumin Protein on Gold Nanoparticles Investigated Using Dimensional Measurements and in Situ Spectroscopic Methods. *Langmuir* **2011**, *27*, 2464−2477.
(53) Lundqvist, M.; Sethson, I.; Jonsson, B. H. Protein Adsorption Onto Silica Nanoparticles: Conformational Changes Depend on the Particles' Curvature and the Protein Stability. *Langmuir* **2004**, *20*, 10639−10647.
(54) Zeng, S.; Huang, M.; Chang, C.-e. A.; Zhong, W. Protein Binding for Detection of Small Changes on Nanoparticle Surface. *Analyst* **2014**, *139*, 1364−1371.
(55) Li, N.; Zeng, S.; He, L.; Zhong, W. Exploration of the Possible Binding Sites of Nanoparticles on Protein. *Anal. Chem.* **2012**, *83*, 6929−6934.